

## Article

# Valorization of Raw and Calcined Chicken Eggshell for Sulfur Dioxide and Hydrogen Sulfide Removal at Low Temperature

Waseem Ahmad <sup>1</sup>, Sumathi Sethupathi <sup>1,\*</sup>, Yamuna Munusamy <sup>1</sup> and Ramesh Kanthasamy <sup>2</sup>

<sup>1</sup> Faculty of Engineering and Green Technology, Universiti Tunku Abdul Rahman, Jalan Universiti, Bandar Barat, Kampar 31900, Perak, Malaysia; waseemssb@gmail.com (W.A.); yamunam@utar.edu.my (Y.M.)

<sup>2</sup> Chemical and Materials Engineering Department, Faculty of Engineering Rabigh, King Abdulaziz University, P.O. Box 344, Rabigh 21911, Saudi Arabia; rsampo@kau.edu.sa

\* Correspondence: sumathi@utar.edu.my; Tel.: +60-54-688-888; Fax: +60-54-667-449

**Abstract:** Chicken eggshell (ES) is a waste from the food industry with a high calcium content produced in substantial quantity with very limited recycling. In this study, eco-friendly sorbents from raw ES and calcined ES were tested for sulfur dioxide (SO<sub>2</sub>) and hydrogen sulfide (H<sub>2</sub>S) removal. The raw ES was tested for SO<sub>2</sub> and H<sub>2</sub>S adsorption at different particle size, with and without the ES membrane layer. Raw ES was then subjected to calcination at different temperatures (800 °C to 1100 °C) to produce calcium oxide. The effect of relative humidity and reaction temperature of the gases was also tested for raw and calcined ES. Characterization of the raw, calcinated and spent sorbents confirmed that calcined eggshell CES (900 °C) showed the best adsorption capacity for both SO<sub>2</sub> (3.53 mg/g) and H<sub>2</sub>S (2.62 mg/g) gas. Moreover, in the presence of 40% of relative humidity in the inlet gas, the adsorption capacity of SO<sub>2</sub> and H<sub>2</sub>S gases improved greatly to about 11.68 mg/g and 7.96 mg/g respectively. Characterization of the raw and spent sorbents confirmed that chemisorption plays an important role in the adsorption process for both pollutants. The results indicated that CES can be used as an alternative sorbent for SO<sub>2</sub> and H<sub>2</sub>S removal.

**Keywords:** chicken eggshell; waste valorization; adsorption; biogas; flue gas



**Citation:** Ahmad, W.; Sethupathi, S.; Munusamy, Y.; Kanthasamy, R.

Valorization of Raw and Calcined Chicken Eggshell for Sulfur Dioxide and Hydrogen Sulfide Removal at Low Temperature. *Catalysts* **2021**, *11*, 295. <https://doi.org/10.3390/catal11020295>

Academic Editor: Daniela Barba

Received: 18 January 2021

Accepted: 19 February 2021

Published: 23 February 2021

**Publisher's Note:** MDPI stays neutral with regard to jurisdictional claims in published maps and institutional affiliations.



**Copyright:** © 2021 by the authors. Licensee MDPI, Basel, Switzerland. This article is an open access article distributed under the terms and conditions of the Creative Commons Attribution (CC BY) license (<https://creativecommons.org/licenses/by/4.0/>).

## 1. Introduction

Sulfur dioxide (SO<sub>2</sub>) and hydrogen sulfide (H<sub>2</sub>S) are both considered toxic gases. SO<sub>2</sub> is mainly part of the flue gases while H<sub>2</sub>S is naturally present in many fossil fuels and quickly oxidizes to SO<sub>2</sub> upon burning. Direct release of these acidic gases to the open air can cause serious environmental repercussions [1,2]. SO<sub>2</sub> can be removed from flue gas in many ways and this process is named as flue gas desulfurization (FGD). The adsorption processes are already used and are well known for SO<sub>2</sub> removal as well as for H<sub>2</sub>S removal. Common sorbents for SO<sub>2</sub> removal are mostly calcium-based oxide/hydroxide (CaO/Ca(OH)<sub>2</sub>), zinc oxide-based (ZnO), sodium hydroxide based (NaOH) and ammonia-based [3]. Limestone, slaked lime or a mixture of slaked lime with fly ash is commercially used in FGD systems [4]. There is a lot of room for improvement in the traditional FGD technologies as they consume a large quantity of water and at times CO<sub>2</sub> leakage to the environment [5,6]. Therefore, recently, many alternative sorbents such as red mud and various modified carbonaceous catalysts, have been developed with the aim to reduce the cost, promote principles of circular economy, and improve energy efficiency [7,8].

The removal of H<sub>2</sub>S, on the other hand, is considered a crucial step in the biogas industry because of its toxic and corrosive nature [9]. Effective utilization of biogas as biomethane is a challenge because of its costly purification steps [10]. Many technologies such as adsorption, alkaline washing (absorption), membrane separation, and cryogenic distillation have been tested to efficiently removes H<sub>2</sub>S [11]. The most common type of sorbent used for adsorption process is impregnated activated carbon [10]. Activated carbon has been reported to have H<sub>2</sub>S removal capacities in the range of 150–650 mg/g [12].

However, adsorption of SO<sub>2</sub> or H<sub>2</sub>S using activated carbon generates secondary waste, which is acidic and difficult for landfilling. Apart from activated carbons, various types of waste-based sorbents derived from municipal waste sludge, fly ash, forestry, slaughterhouse, etc. have been also tested for H<sub>2</sub>S removal [10]. Nevertheless, these sorbents are either not re-generable or has a very low removal efficiency. Thus, recently researchers are focusing on developing new cost-effective and regenerative sorbents for H<sub>2</sub>S removal.

Chicken eggshell (ES) is a waste product from the food industry and is mostly disposed in landfills in Malaysia. It contains about 90–95% of calcium carbonate in the form of calcite, 1% magnesium carbonate, 1% calcium phosphate and some organic compounds [13,14]. According to Food and Agriculture Organization (FAO) of the United Nations, approximately 70.4 million tons of chicken eggs were produced worldwide in 2015 and the production is estimated to increase to 90 million tons by 2030 [15]. In Malaysia, about 642,600 tonnes of chicken eggs are produced annually which produces approximately 70,686 tonnes of ES waste [16]. Considering the volume of ES waste produced, its reutilization is still very limited and a greater part of it is disposed in landfills. ES has been reported to be used occasionally as a soil conditioner, fertilizer, and additive for animal feed [17]. Recently in the literature, ES waste has been valorized in many innovative applications such as special materials for bone tissue restoration, as a sorbent for metal ions in wastewater treatment and also as a catalyst in different applications [18]. Recently, ES based sorbent was used for CO<sub>2</sub> adsorption and the removal capacity was reported as 10.47 mg/g at 1 bar and 30 °C [19]. Sethupathi et al. (2017) had also carried out a preliminary study on the SO<sub>2</sub> removal from the gaseous stream using CES (950 °C) and achieved maximum adsorption capacity of 2.15 mg/g [20]. One of the latest literatures reported a carbonized hybrid sorbent (ES and lignin) to remove SO<sub>2</sub> from the air [21]. In this study, the possibility of replacing conventional calcite-based sorbents with raw and calcined chicken eggshell for acidic gases removal at low temperature was appraised. Adsorption experiments were conducted in a lab-scale adsorption rig and SO<sub>2</sub> and H<sub>2</sub>S were mixed with nitrogen gas with fixed concentration separately. Various characterization techniques like FTIR, XRD, EDX, and FESEM were used to further investigate the adsorption mechanism.

## 2. Results and Discussions

### 2.1. Characterization of Raw and Calcined Eggshell before and after Adsorption Tests

The morphology of ES sorbents was examined with Field Emission Scanning Electron Microscope (FESEM) images. Figure 1a shows the outer shell of ES and its FESEM images at different magnification. It can be seen that the outer shell of ES has a smooth surface with cracks. Figure 1b is the inner ES with the membrane. FESEM images clearly show fibrous network morphology of protein which is very porous in nature. Figure 1c shows the actual image of powdered (<90 µm) raw eggshell (RES) and FESEM images at different magnification. The porous nature of RES can be clearly seen with the pore hole like structures on the particles. Pore structures of ES sorbents are categorized as Type II as per Brunauer, Deming and Teller classification, stating their characteristics belong to macroporous material, nonporous materials, or materials with open voids.

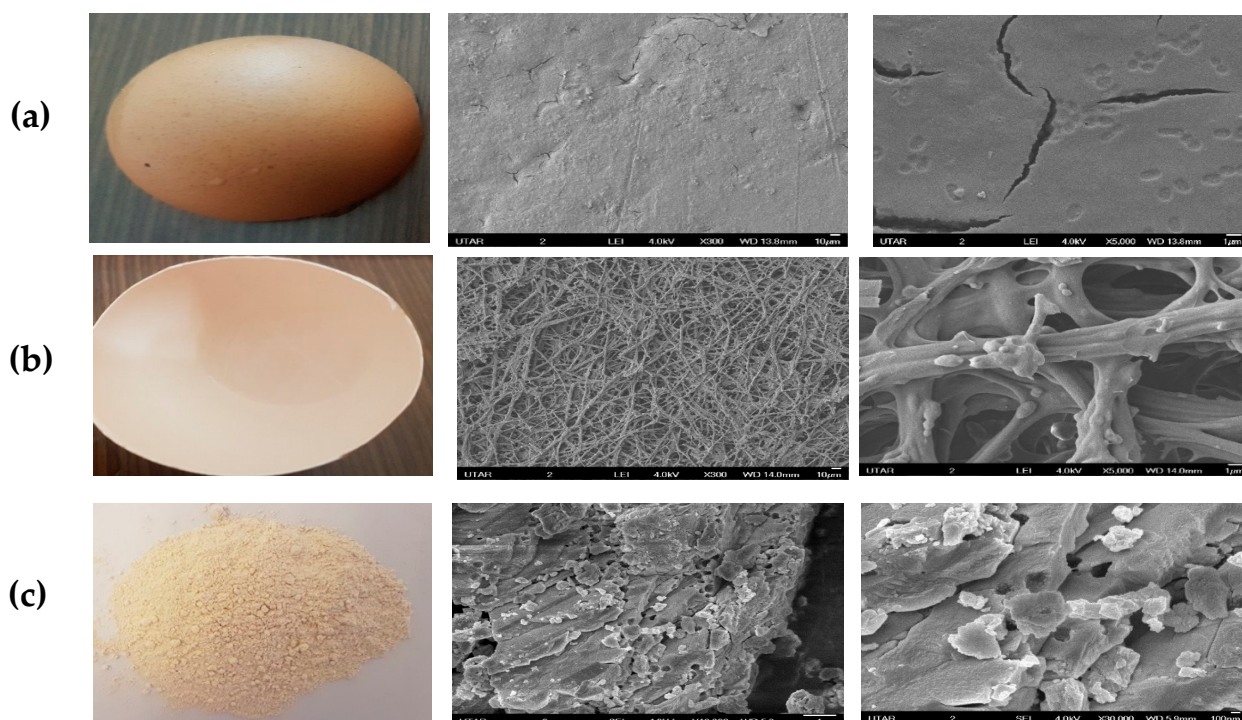


**Figure 1.** Digital camera and FESEM images of raw eggshell. (a) Outer at 300 $\times$  and 5000 $\times$  magnification, (b) inner at 300 $\times$  and 5000 $\times$  magnification, and (c) particle size of  $<90 \mu\text{m}$  at 10,000 $\times$  and 30,000 $\times$  magnification.

Figure 2a,b show FESEM images of (CES 900  $^{\circ}\text{C}$ ) and (CES 1100  $^{\circ}\text{C}$ ). The images for 900  $^{\circ}\text{C}$  show a stable and structured particle compared to the one calcined at 1100  $^{\circ}\text{C}$ . (CES 900  $^{\circ}\text{C}$ ) shows well-arranged particles with smooth surfaces on each particle. (CES 1100  $^{\circ}\text{C}$ ) was totally the opposite, particles lose their shapes, and each particle shows intensive surface cracks due to the sintering process.

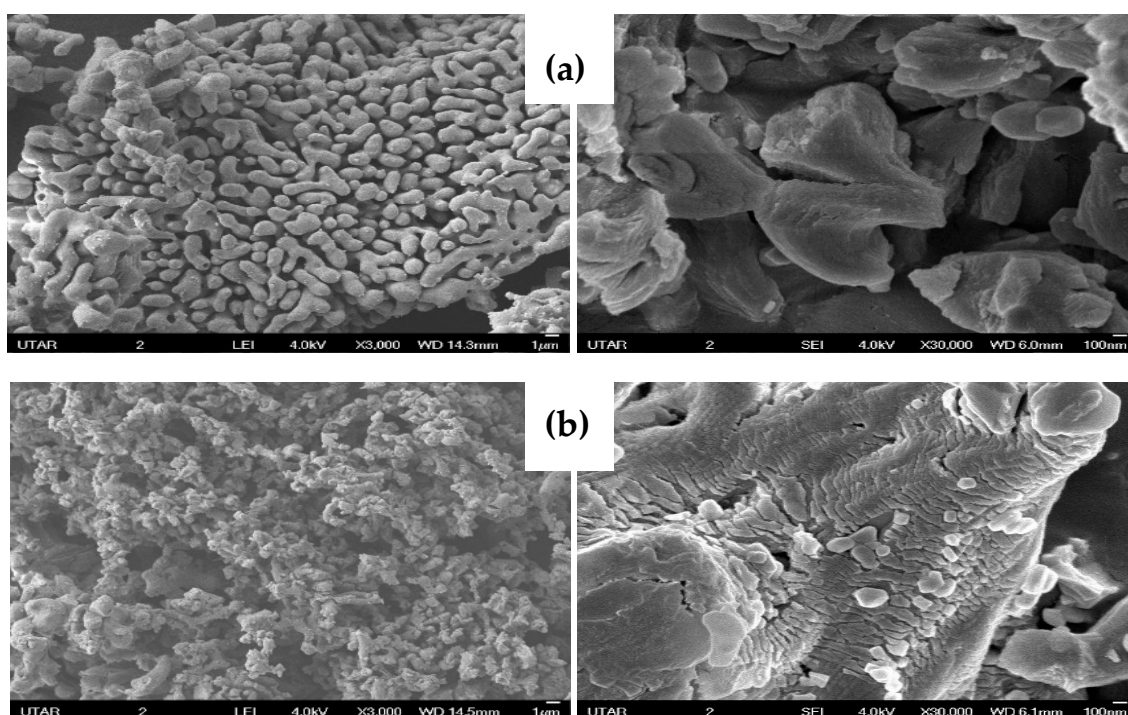


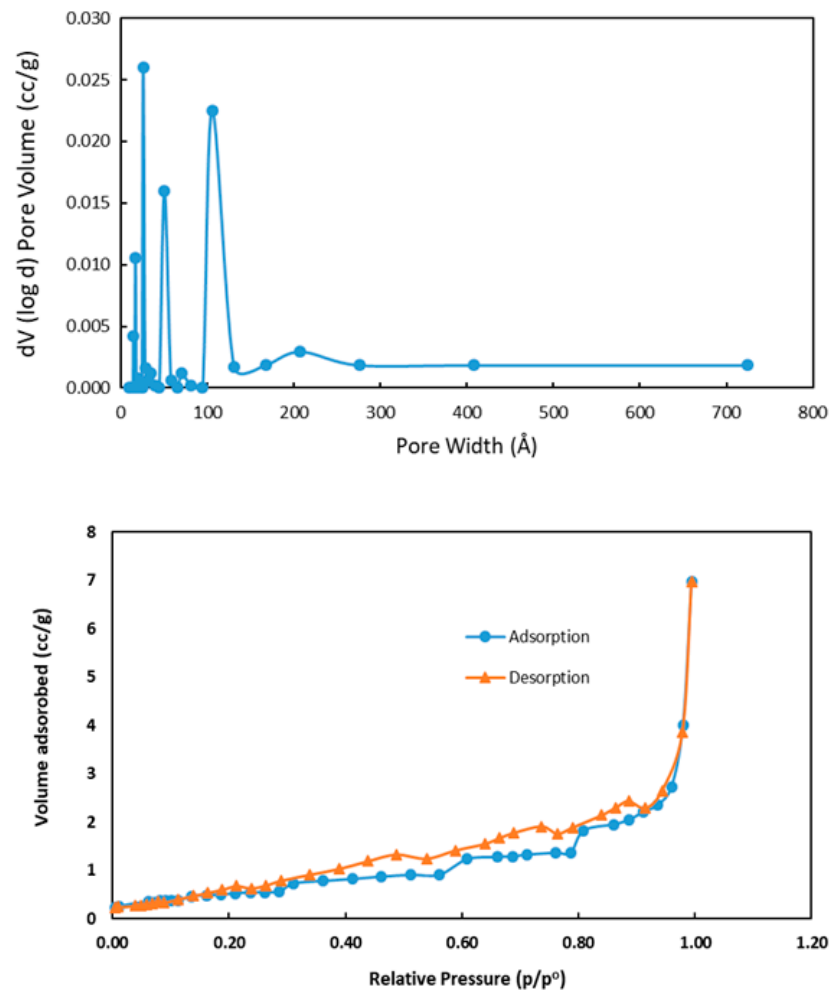
**Figure 2.** FESEM images of calcined eggshell at (a) 900  $^{\circ}\text{C}$  and (b) 1100  $^{\circ}\text{C}$  with 3000 $\times$  and 30,000 $\times$  magnification.

BET surface area values of the CES sorbents in comparison to RES are shown in Table 1. BET surface area of RES was reported as  $0.56 \text{ m}^2/\text{g}$  and the readings were increasing as RES was calcined. However, the values decrease when the temperature was further increased up to  $1000 \text{ }^\circ\text{C}$  and  $1100 \text{ }^\circ\text{C}$ . The highest BET surface area of  $6.74 \text{ m}^2/\text{g}$  was recorded at  $900 \text{ }^\circ\text{C}$ . The BET surface area of CES was low compared to commercial-grade CaO whose BET surface area is in the range of  $11\text{--}25 \text{ m}^2/\text{g}$  [22].

**Table 1.** BET surface area of calcined eggshell at different temperature.

Calcination Temperature ( $^\circ\text{C}$ )	BET Surface Area ( $\text{m}^2/\text{g}$ )
800	2.98
900	6.74
950	6.54
1000	6.30
1100	2.68

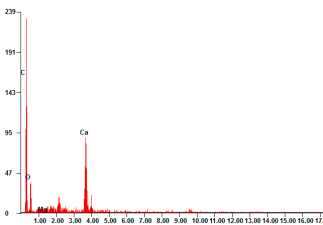
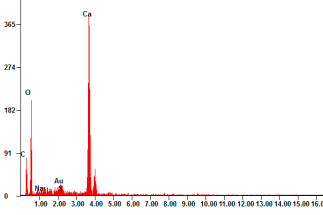
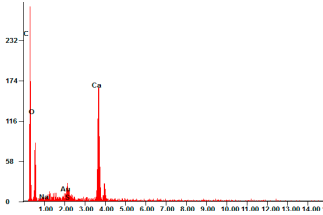
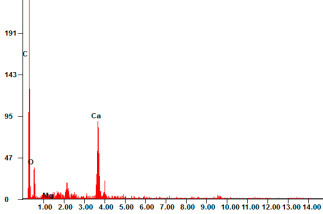
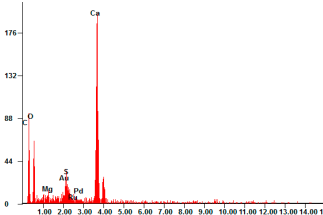
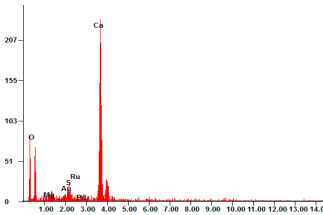
Figure 3 shows the nitrogen-adsorption isotherm for CES. The isotherm is of Type IV. As per IUPAC standard, this kind of isotherm is obtained for a combination of microporous and mesoporous structure which is formed at a higher relative pressure. The low BET surface area of CES could be due to eggshell structure and impurities.



**Figure 3.** Pore size distribution and  $\text{N}_2$  adsorption-desorption isotherm of (CES  $900 \text{ }^\circ\text{C}$ ).

The elemental content of RES, CES, and their respective spent sorbents are shown in Table 2. The presence of the sulfur element in the spent RES and CES affirms the adsorption of SO<sub>2</sub> and H<sub>2</sub>S and the occurrence of chemisorption.

**Table 2.** The differences in elemental content of raw eggshell and (CES 900 °C) before and after adsorption.

Sample	EDX Figure	Elements	Percentage
RES		Ca C O Others	16.85 31.80 49.13 2.22
RES Spent SO <sub>2</sub>		Ca C O S Others	12.08 27.68 57.84 0.55 1.85
RES Spent H <sub>2</sub> S		Ca C O S Others	11.35 56.25 30.95 0.11 1.34
(CES 900 °C)		Ca C O Others	24.93 35.87 38.23 0.47
(CES 900 °C) Spent SO <sub>2</sub>		Ca C O S Others	14.65 41.33 42.4 0.65 1.06
(CES 900 °C) Spent H <sub>2</sub> S		Ca C O S Others	16.05 36.8 46.25 0.21 0.69

The Ca content in the CES is more compared to the one in raw eggshell (RES) because, during the calcination, CO<sub>2</sub> and other volatile matters are released. It is also evident that the contents of other impurities in ES such as Zn, Mg, Al, and Cu remain almost the same in RES, CES and spent sorbents. This shows that these impurities were not involved in the

sorption process. In the spent adsorbent, the content of Ca was reduced. This indicated the conversion of Ca into sulfite complex.

FTIR spectra of RES, (CES 900 °C) and the spent sorbents are presented in Figure 4. The wideband approximately at 3430  $\text{cm}^{-1}$  in the RES is attributed to the stretching of the OH bond [23]. The two well-defined bands at 1413  $\text{cm}^{-1}$  and 874  $\text{cm}^{-1}$  are distinctive to the bending of C–O bond of  $\text{CaCO}_3$  while the band at 712  $\text{cm}^{-1}$  is related to Ca–O bond [24]. These indicate that RES comprises of calcite [25]. For (CES 900 °C), the well-defined band at approximately 3630  $\text{cm}^{-1}$  corresponds to the vibration of OH bonds probably attached to the surface of CaO [24]. The peak at 1413  $\text{cm}^{-1}$  is sharper in (CES 900 °C) showing a higher percentage of CaO and more prevailing than RES. New peaks were not detected in the spent RES sorbents. Nevertheless, there were changes in the intensity of the peaks. This could be due to the contact of the acidic gases. However, a new peak at 1080  $\text{cm}^{-1}$  was visible for (CES 900 °C) spent sorbents. This affirms the presence of sulfite [26].

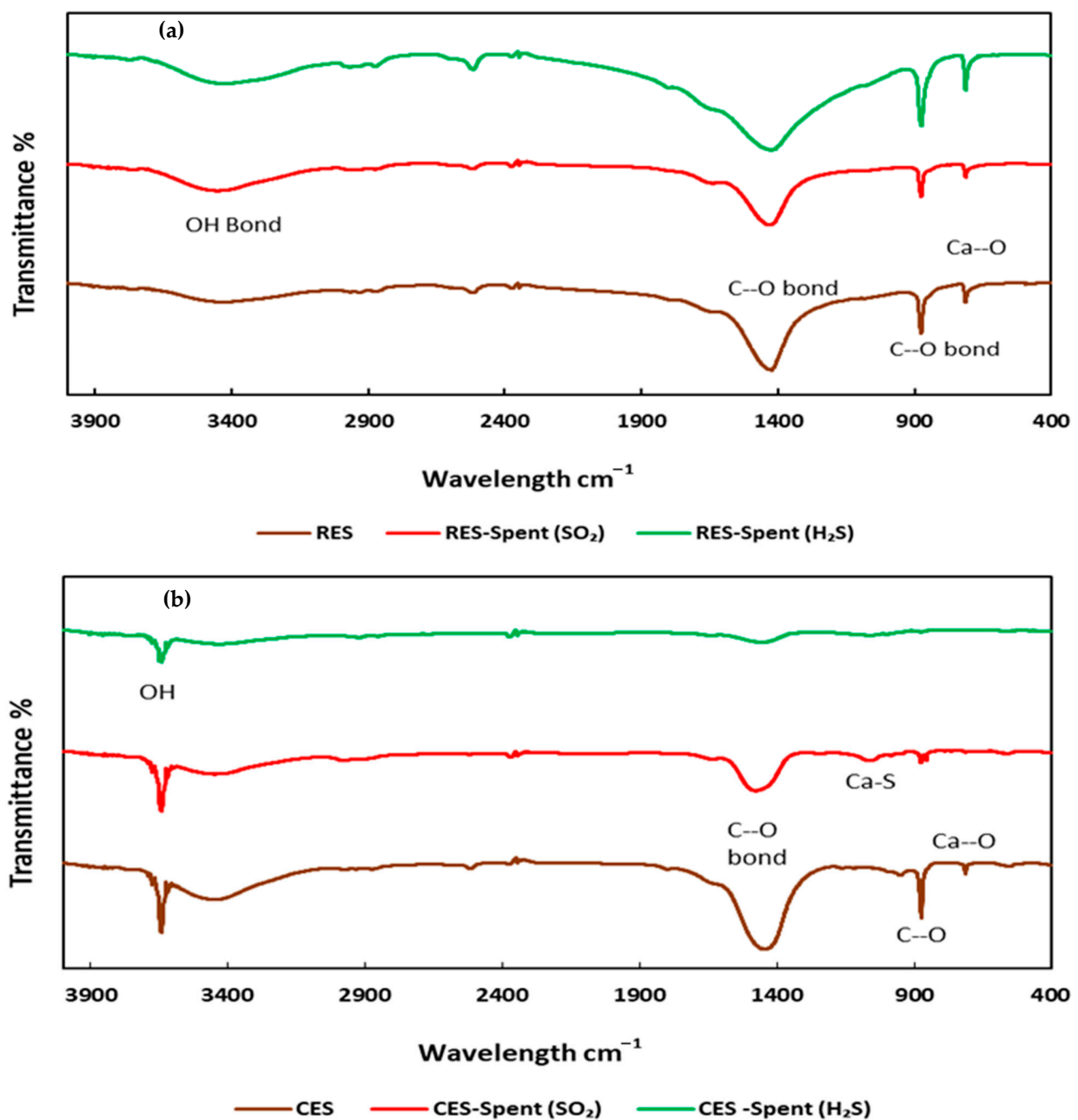


Figure 4. FTIR spectra of (a) raw eggshell and (b) calcined eggshell (900 °C) before and after adsorption.

The proximate analyses of RES and CES are listed in Table 3. The moisture content and volatile matter of CES were much lesser than RES due to the high-temperature calcination process. The residue for CES was far greater than RES which shows the stability of CES at high temperature and amount of CaO produced.

**Table 3.** Proximate analysis of raw and calcined eggshell (900 °C).

Temperature (°C)	Proximate Analysis	RES (%)	CES (%)
25–120	Moisture	1.03	0.28
120–450	Volatile content	4.18	8.01
450–800	CO <sub>2</sub>	43.17	1.63
800–900	Residue (CaO)	51.62	90.08

Figure 5 show X-ray diffraction (XRD) of RES, (CES 900 °C) and the spent sorbents. RES showed a major peak at  $2\theta = 29.5^\circ$  which indicates that CaCO<sub>3</sub> is a major constituent of the waste ES. In the (CES 900 °C), regular peaks were obtained at  $2\theta = 32^\circ, 34^\circ, 37.5^\circ,$  and  $54^\circ$ , showing the conversion of CaCO<sub>3</sub> to CaO [23]. It is noted that peak at  $2\theta = 29.5^\circ$  is no longer visible in the (CES 900 °C), which implies a complete conversion of CaCO<sub>3</sub> to CaO.

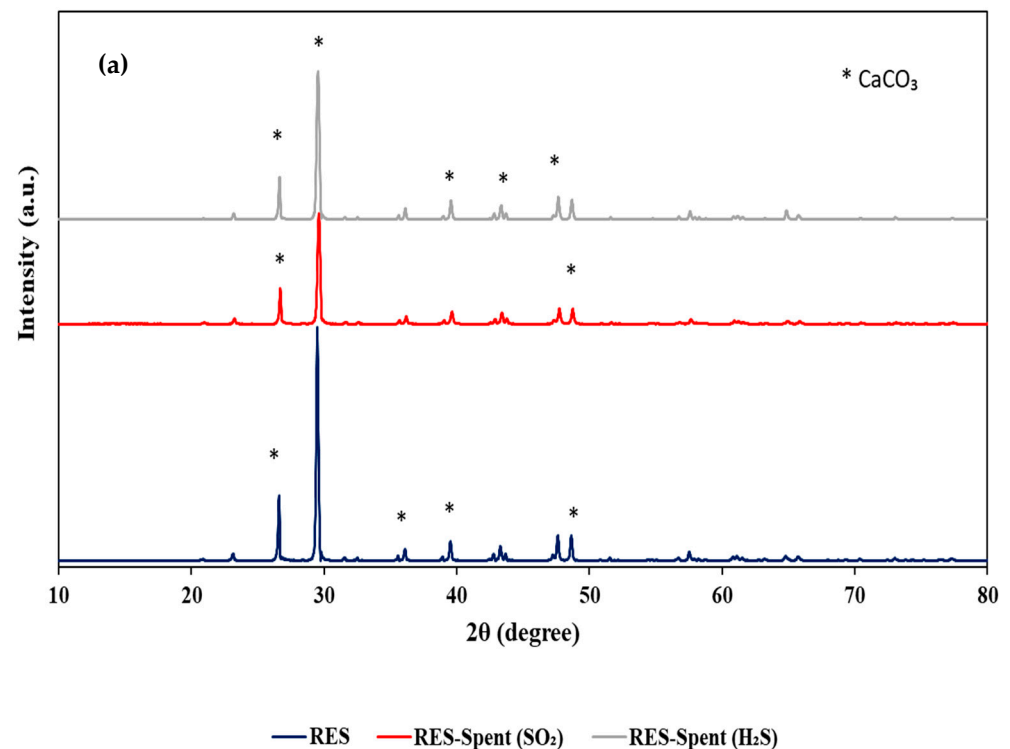


**Figure 5.** Cont.

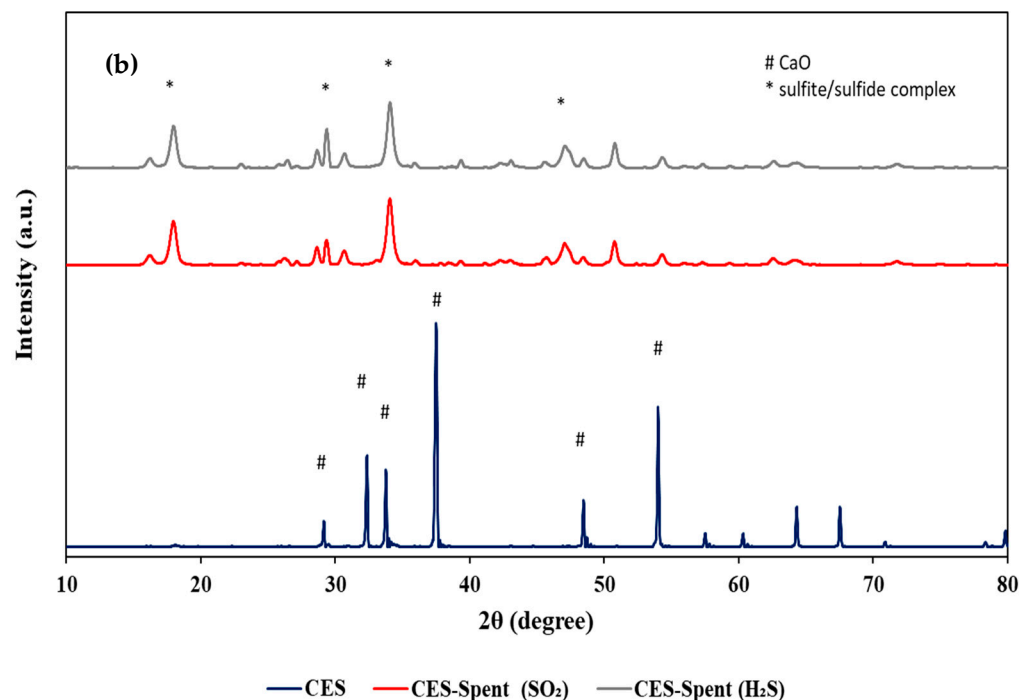


**Figure 5.** XRD pattern of (a) raw eggshell and (b) calcined eggshell (900 °C) before and after adsorption.

For the spent RES, it can be seen that there was no significant difference in the crystalline structure after the adsorption of  $\text{SO}_2$  and  $\text{H}_2\text{S}$ . It shows no chemical interaction between the sorbent and the gases. Thus, it can be concluded that for RES the adsorption was merely physical. However, for spent (CES 900 °C), the initial peaks at  $2\theta = 32^\circ$ ,  $34^\circ$ ,  $37.5^\circ$ , and  $54^\circ$  have disappeared and new peaks were formed at  $2\theta = 17^\circ$  and  $29^\circ$ . The peak at  $34^\circ$  in the (CES 900 °C) corresponds to CaO. This peak reduced in the spent sorbent, indicating the presence of unreacted CaO in the spent sorbent. The small peaks at  $2\theta = 17^\circ$ ,  $28^\circ$ ,  $28^\circ$ , and  $2\theta = 34^\circ$ ,  $47^\circ$ ,  $52^\circ$ , and  $54^\circ$  may correspond to  $\text{CaSO}_3$  and  $\text{Ca}(\text{OH})_2$  respectively for the spent (CES 900 °C). These spread-out peaks show that the crystallinity of (CES 900 °C) after adsorption has dropped. Similar peaks were reported by others as well [27].

pH values of the RES and CES before and after adsorption are tabulated in Tables 4 and 5 to show the reactivity of the acidic gases on RES and CES. There was a clear increase in pH with the increase in calcination temperature because of the formation of CaO which is basic in nature. Whereas for RES, the sorbents with membrane have slightly higher pH compared to the one without membrane. This is due to the different types of protein in the membrane. It was noticed that for all cases, spent sorbent's pH values dropped one level, indicating successful adsorption of acidic gases.

**Table 4.** Adsorption capacity and saturation time of raw eggshell with and without membrane at different particle size.

Sample	Particle Size ( $\mu\text{m}$ )	Saturation Time (min)		Adsorption Capacity (mg/g)		Original pH	pH (after Adsorption)	
		$\text{SO}_2$	$\text{H}_2\text{S}$	$\text{SO}_2$	$\text{H}_2\text{S}$		$\text{SO}_2$	$\text{H}_2\text{S}$
Raw eggshell with membrane	<90	32.2	44.0	1.09	0.65	$9.2 \pm 0.2$	$8.7 \pm 0.2$	$8.9 \pm 0.2$
	90–125	29.0	20.5	0.89	0.19			
	125–180	15.3	8.0	0.61	0.08			
Raw eggshell without membrane	<90	29.8	33.0	0.98	0.26	$8.9 \pm 0.2$	$8.4 \pm 0.2$	$8.6 \pm 0.2$
	90–125	25.5	17.5	0.66	0.14			
	125–180	13.3	7.5	0.54	0.05			

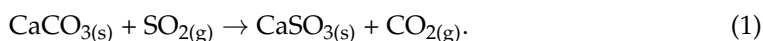
**Table 5.** Adsorption capacity and pH of calcined eggshell at different temperature.

Calcination Temperature (°C)	BET Surface Area (m <sup>2</sup> /g)	Adsorption Capacity (mg/g)		Original pH	pH (After Adsorption)	
		SO <sub>2</sub>	H <sub>2</sub> S		SO <sub>2</sub>	H <sub>2</sub> S
800	2.98	2.12	1.30	10.9 ± 0.2	10.1 ± 0.2	10.3 ± 0.2
900	6.74	3.53	2.62	11.8 ± 0.2	10.9 ± 0.2	11.1 ± 0.2
950	6.54	3.22	2.35	12.0 ± 0.2	11.2 ± 0.2	11.4 ± 0.2
1000	6.30	2.69	1.85	12.1 ± 0.2	11.3 ± 0.2	11.5 ± 0.2
1100	2.68	2.55	1.66	12.3 ± 0.2	11.4 ± 0.2	11.5 ± 0.2

## 2.2. Effect of the Eggshell Membrane and Particle Size

Three different particle sizes (<90 µm, 90–125 µm, and 125–180 µm) of RES with and without membrane were tested for the SO<sub>2</sub> and H<sub>2</sub>S removal. During this analysis, other parameters such as sorbent dosage (1 g), flow rate (300 mL/min), humidity (0%), gas inlet concentration (300 ppm), pressure (1 bar), and reaction temperature (ambient temperature, 29 °C) were all kept constant. Table 4 shows the adsorption capacity and saturation time of SO<sub>2</sub> and H<sub>2</sub>S adsorption by RES with and without membrane. It was noticed that for both H<sub>2</sub>S and SO<sub>2</sub> the adsorption capacities were less than 1.1 mg/g on dry basis. The breakthrough point was not detected which indirectly shows that there was no immediate chemical interaction between the gas and sorbent. It is known that CaCO<sub>3</sub> is a highly stable material at ambient conditions. Thus, RES with or without membrane could have similar behavior. RES with membrane recorded higher adsorption capacity and longer saturation time for both H<sub>2</sub>S and SO<sub>2</sub> gas compared to the one without membrane. According to Tsai et al. (2006), ES membrane comprises of a grid of fibrous proteins which contributes to its large surface areas and these fibrous proteins have higher BET surface area compared to the shell itself [28]. In the literature, the role of ES membrane in the removal of reactive dyes, heavy metals, phenols, and various other substances was reported and in most of the cases, it was reported that the adsorption capacity was better with membrane compared to one without membrane [29,30]. Thus, in this study, it was found that RES with membrane enhanced the sorption of H<sub>2</sub>S and SO<sub>2</sub>.

As for the effect of particle size, as anticipated, the smallest particle size i.e., <90 µm shows the best results for both RES with and without membrane. The calculated adsorption capacity values followed the following sequence for both gases: 90 µm > 125 µm > 180 µm. Witoon (2011) had stated that the smaller particle size of calcined ES had higher CO<sub>2</sub> capture capacity because it provides a greater exposed surface for the adsorption [23]. Similarly, in this study, smaller particles can offer a greater surface area for gas–solid interactions. The macro-pores and pits are irregularly dispersed over the surface of the RES, which could be one of the factors for low adsorption capacity as evident from the FESEM image. At high temperature, CaCO<sub>3</sub> breaks down to CaO<sub>(s)</sub> and release CO<sub>2</sub>. The Ca<sup>+2</sup> of CaO is unstable and reacts with SO<sub>2(g)</sub> replacing oxygen at high temperature. The reaction of SO<sub>2</sub> gas on CaCO<sub>3</sub> can be shown by the following chemical reaction [31];

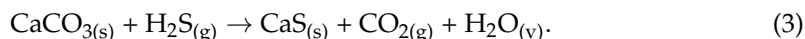


However, calcium sulfate (CaSO<sub>4</sub>) is only formed from the reaction between calcium carbonate (CaCO<sub>3</sub>) and SO<sub>2</sub> gas when the temperature is more than 750 K in presence of oxygen (O<sub>2</sub>) as illustrated below [31];



As the experiments were carried out in room temperature and O<sub>2</sub> was not induced in this study, the only possible reaction would be the formation of calcium sulfite (CaSO<sub>3</sub>)

rather than  $\text{CaSO}_4$ . For the reaction between  $\text{CaCO}_3$  of RES and  $\text{H}_2\text{S}$ , the following direct sulfidation reaction is expected [32]:



However, at room temperature,  $\text{CaCO}_3$  is very stable and the chances of the above reactions are very slim. However, for RES only physical adsorption has happened for both  $\text{SO}_2$  and  $\text{H}_2\text{S}$  which is the main reason for its low adsorption capacities. As physical adsorption is happening, so the particle size and surface porosity played an important role.

### 2.3. Effect of Calcination Temperature

The influence of various calcination temperature on RES and their effect on  $\text{SO}_2$  and  $\text{H}_2\text{S}$  adsorption were tested using dried and powdered ( $<90 \mu\text{m}$ ) RES with membrane. Other adsorption parameters were kept the same as in section "Effect of the eggshell membrane and particle size". Figure 6a,b shows the breakthrough curves of  $\text{SO}_2$  and  $\text{H}_2\text{S}$  versus calcination temperature of ES. Among the calcination temperature,  $900^\circ\text{C}$  shows a prominent outstanding curve. Breakthrough points were very short however, it has a longer saturation time (84 min and 77 min for  $\text{SO}_2$  and  $\text{H}_2\text{S}$ , respectively) for both gases.

Table 5 tabulates the adsorption capacity of the CES at different temperatures. (CES  $900^\circ\text{C}$ ) shows the highest adsorption capacity i.e., 2.63 mg/g and 3.53 mg/g for  $\text{H}_2\text{S}$  and  $\text{SO}_2$  respectively. High adsorption capacity at  $900^\circ\text{C}$  calcination could be due to the complete conversion of calcium carbonate ( $\text{CaCO}_3$ ) to calcium oxide ( $\text{CaO}$ ). It is noted that complete conversion takes place around  $930^\circ\text{C}$  [32,33]. Thus, at temperature  $800^\circ\text{C}$ , lower adsorption capacity was noticed for both gases. Moreover, the  $800^\circ\text{C}$  calcined ES was visibly grayish in color compared to the ones calcined at a higher temperature which were whitish confirming the incomplete calcination. At higher temperature i.e.,  $>900^\circ\text{C}$ , the adsorption capacities for both  $\text{SO}_2$  and  $\text{H}_2\text{S}$  decreased. Moreover, the saturation time was shorter and there was no breakthrough point. The decrease in adsorption capacity is due to the sintering effect. Similar work on  $\text{SO}_2$  adsorption by calcined limestone reported that pore size distribution is greatly affected by the calcination temperature.

It was reported that  $950^\circ\text{C}$  was the optimized calcination temperature for limestone and at this temperature, the pores of  $\text{CaO}$  have the least diffusion resistance and highest activity for  $\text{SO}_2$  removal [34]. Another similar work mentioned that sintering of  $\text{CaO}$  derived from pure  $\text{CaCO}_3$  starts at  $800\text{--}900^\circ\text{C}$  and it becomes more severe after  $950^\circ\text{C}$ . ES is less pure than the commercial limestone, where for each 100 g of air-dried of ES waste only 88 g are of  $\text{CaCO}_3$  [35], which corresponds to an increase in the rate of sintering [36,37]. Also, it was proven that a breakdown of the pores occurs for  $1100^\circ\text{C}$ . These statements can be confirmed using BET surface area readings, and FESEM images.

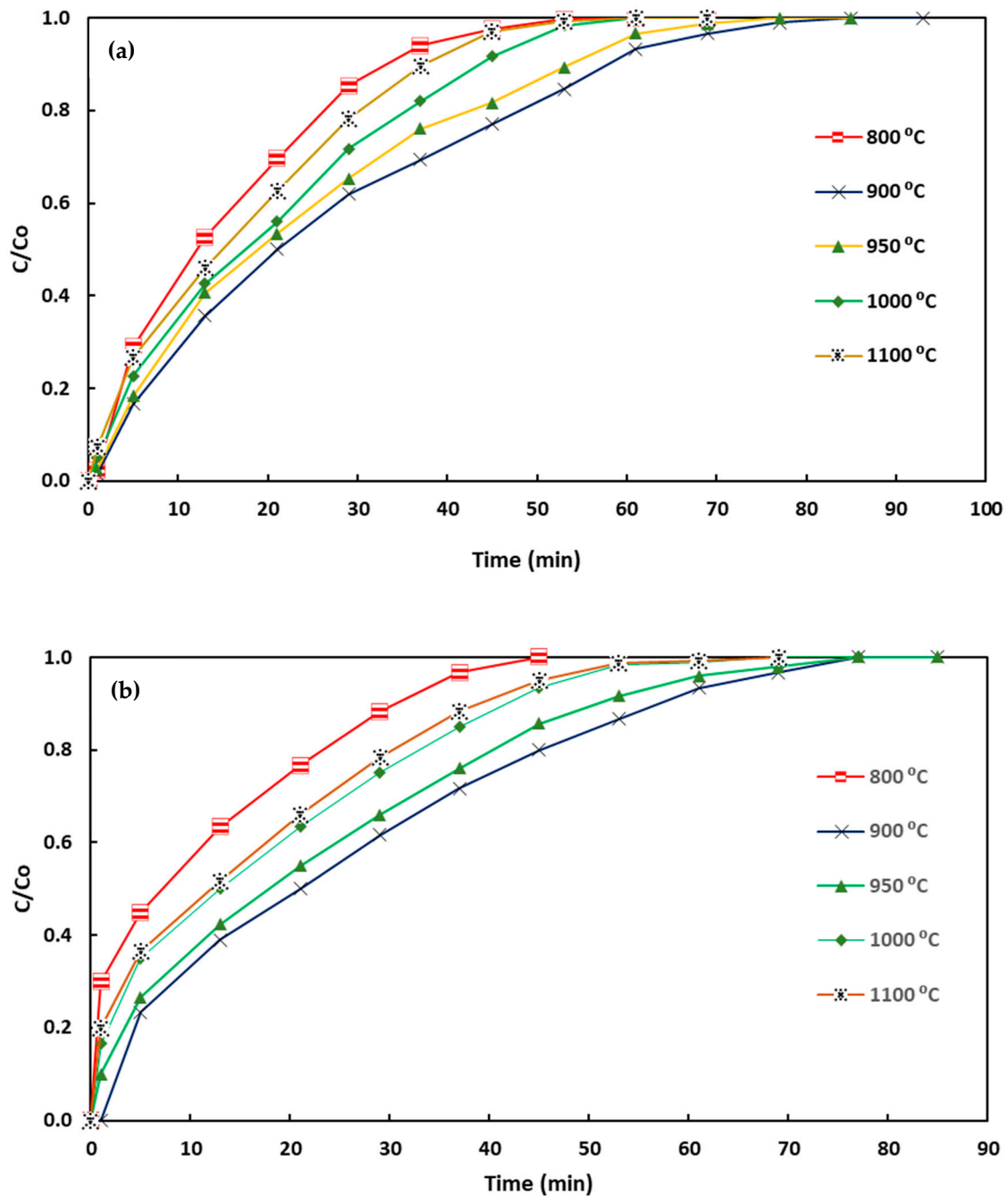


Figure 6. Adsorption breakthrough curves of (a)  $\text{SO}_2$  and (b)  $\text{H}_2\text{S}$  by eggshell at different calcination.

#### 2.4. Effect of Reaction Temperature and Humidity

The influence of reaction temperature on  $\text{SO}_2$  and  $\text{H}_2\text{S}$  adsorption by RES and (CES 900 °C) was evaluated using two different reactor temperatures (100 °C and 200 °C). Other parameters such as sorbent dosage (1 g), flow rate (300 mL/min), gas inlet concentration (300 ppm), and pressure (1 bar) were all kept constant. Table 6 shows the adsorption capacity for the effect of reaction temperature and humidity. Figure 7 shows the breakthrough curve for the effect of reaction temperature on  $\text{H}_2\text{S}$  and  $\text{SO}_2$  removal. The trend was comparatively better than the ones done at the room temperature (29 °C) earlier. However, the impact was very minimal for (CES 900 °C). Meanwhile, for RES, the adsorption capacity was doubled when the reactor temperature was increased from 30 °C to 200 °C. It was claimed that an increase in reaction temperature, increases the chemical interaction of  $\text{SO}_2$  and  $\text{H}_2\text{S}$  with limestone-based  $\text{CaCO}_3$  or  $\text{CaO}$  or  $\text{Ca}(\text{OH})_2$  sorbents [38–40]. The effects

of reactor temperature in the range of room temperature to 200 °C is considered low in magnitude. At a temperature below 200 °C, only calcium sulfite will be formed during the reaction of SO<sub>2</sub> with CaCO<sub>3</sub> and CaO [41]. Calcium sulfite, however, is stable at around 200 °C and only becomes unstable at a temperature above 727 °C decomposing to form calcium sulfate and calcium carbide [42]. Though, at a temperature above 100 °C the rate of calcium sulfite formation tends to increase [41]. There are limited data on SO<sub>2</sub> and H<sub>2</sub>S by CaCO<sub>3</sub> and CaO at temperature < 250 °C. Most of the studies have been done at elevated temperatures, i.e., >400 °C.

**Table 6.** Adsorption capacity of raw and calcined (900 °C) eggshell at different reaction temperature and 40% relative humidity.

Reaction Condition	Raw Eggshell (mg/g)		Calcined Eggshell (900 °C) (mg/g)	
	SO <sub>2</sub>	H <sub>2</sub> S	SO <sub>2</sub>	H <sub>2</sub> S
Reaction Temperature (100 °C)	1.43	0.77	3.93	3.37
Reaction Temperature (200 °C)	2.03	1.20	4.30	4.22
Humidity (40%)	8.89	1.42	11.68	7.96

These analyses illustrated that there are some interactions between SO<sub>2</sub> and H<sub>2</sub>S with RES and CES even at low temperature. A lower temperature will be favorable for SO<sub>2</sub> and H<sub>2</sub>S removal because the temperature of flue gas going to the stack is around 150 °C and the working temperature of is about 55 °C [43,44]. However, at a higher temperature, the reaction could be further enhanced. A study of SO<sub>2</sub> adsorption by lime (80% CaO) reported that the conversion rate gets double when the temperature increases from 400 °C to 800 °C [45]. Moreover, during the reaction of CaCO<sub>3</sub> with H<sub>2</sub>S, complete conversion of CaCO<sub>3</sub> to CaS is only feasible if sulfidation is carried out at a temperature above its calcination temperature [46]. Thus, it can be concluded that a more conducive environment is created for the sulfidation of both RES and (CES 900 °C) by increasing the reaction temperature up to 200 °C.

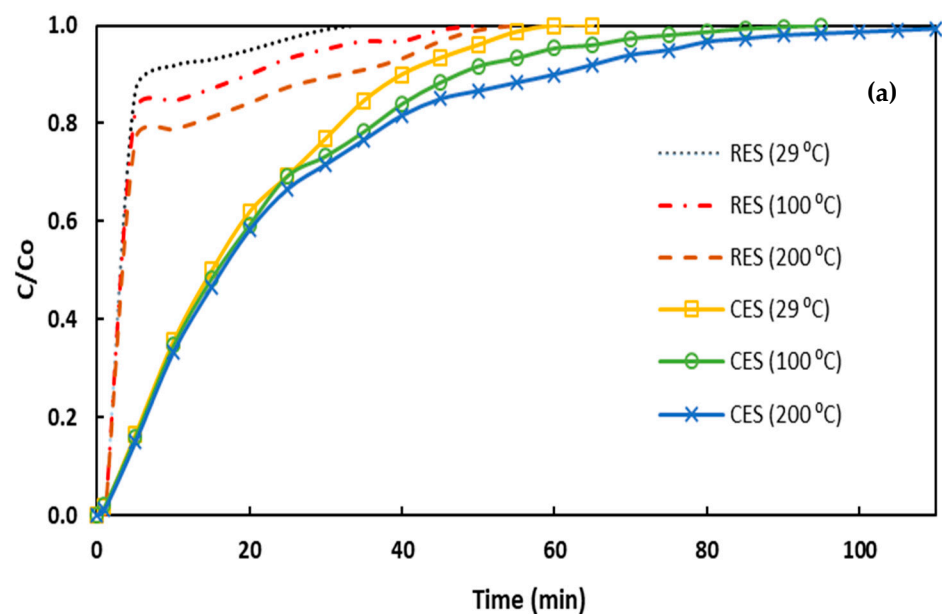


**Figure 7.** Cont.

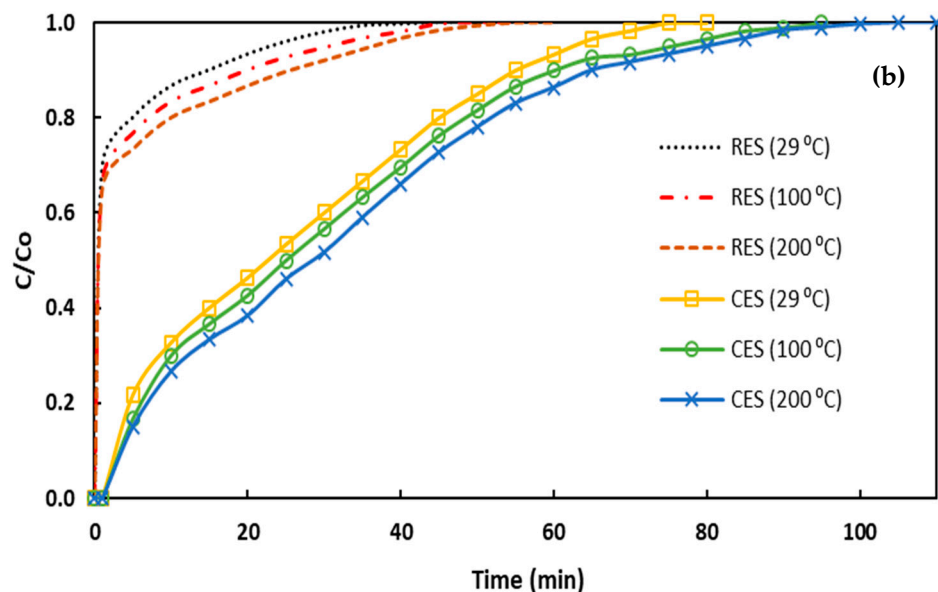
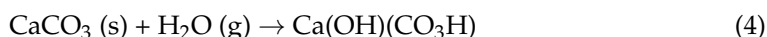


Figure 7. Breakthrough curves of (a) SO<sub>2</sub> and (b) H<sub>2</sub>S at different reaction temperature.

Figure 8 shows the breakthrough curves of RES and (CES 900 °C) with a response to the effect of humidity. All other parameters were kept constant. It was noticed that with the addition of 40% relative humidity (RH), the performance of both RES and (CES 900 °C) improved significantly. The adsorption capacity of SO<sub>2</sub> and H<sub>2</sub>S by (CES 900 °C) increased almost triple with humidity. There were significant improvements in the breakthrough time as well as saturation time for both SO<sub>2</sub> and H<sub>2</sub>S. The breakthrough point was clearly noticeable for (CES 900 °C). For RES, a great increase was noticed for SO<sub>2</sub>, however, for H<sub>2</sub>S, only small improvement was noticed. Results can be compared from Tables 4–6. The presence of humidity in the inlet gas improved the adsorption capacity of SO<sub>2</sub> more than the H<sub>2</sub>S for RES. This could be due to the solubility of SO<sub>2</sub>. The solubility of SO<sub>2</sub> in water is about 16 times more than the solubility of H<sub>2</sub> as per the data published by [47]. The chemical reaction of SO<sub>2</sub> and CaCO<sub>3</sub> in the presence of RH is as shown below;



Carbonic acid (H<sub>2</sub>CO<sub>3</sub>) is a product of this surface reactions, not alike the one without RH which produces carbon dioxide [31]. Between 30% and 85% RH, SO<sub>2</sub> and CaCO<sub>3</sub> reaction are improved significantly, approximately by 5 to 10 fold for single crystal CaCO<sub>3</sub> (calcite) in the presence of moisture [48]. A slight improvement is noticed because of the humidity which made the contact possible between CaCO<sub>3</sub> and the acidic gases [49]. It is known that CaO reaction in the presence of water vapor will form Ca(OH)<sub>2</sub>. At low temperature, it is expected that only sulfite hemihydrate will be formed when SO<sub>2</sub> is present [41]. The following reaction could occur;



The chemisorption process of SO<sub>2</sub> onto the sorbent surface as described Equation (6) chemical reaction increases with increasing RH [41]. It has been reported that moisture can enhance the adsorption capacity of carbonates and oxides for atmospheric gases [31]. For example, in a humid air condition, the deposition velocity of SO<sub>2</sub> gas onto calcite and dolomite increases [31]. Moreover, SO<sub>2</sub> can oxidize to SO<sub>3</sub>, to form sulfuric acid [50]. Similarly, for H<sub>2</sub>S, there was a small increase in the adsorption capacity although the gas is not readily soluble in water. This increase is attributed to the contact time between CaO sorbent and water vapor. H<sub>2</sub>S partly dissolves in water to form a weak acid and CaO would

readily attract a water molecule to convert to a more stable form of calcium hydroxide (CaOH)<sub>2</sub>. Yet, the chances of additional reaction between CaOH and H<sub>2</sub>S to form CaS are low as this reaction could only happen at high temperature, i.e., above 900 °C [51].

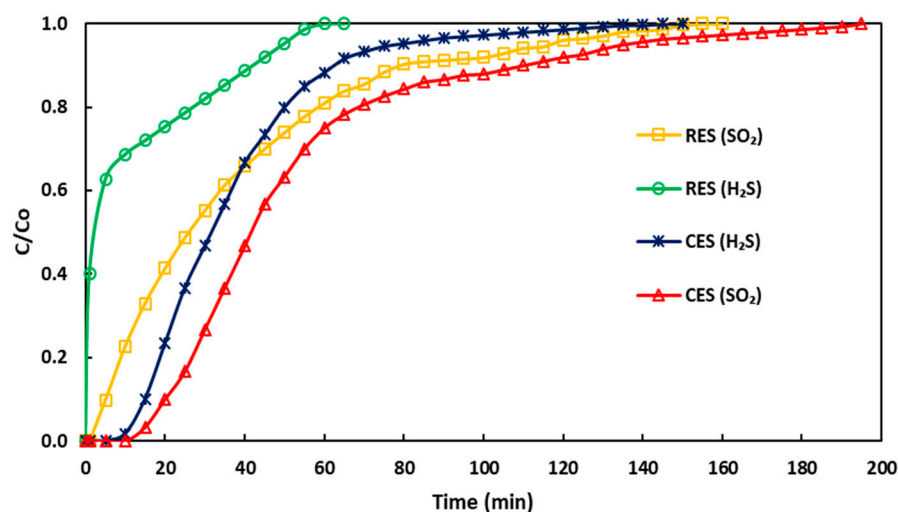


Figure 8. Breakthrough curves of SO<sub>2</sub> and H<sub>2</sub>S with 40% relative humidity.

### 2.5. Comparison Study

Table 7 shows a comparison of various sources of Ca-based sorbents and its potential to adsorb SO<sub>2</sub> and H<sub>2</sub>S respectively. It can be seen that the adsorption capacity of the CES is comparable to that of the Ca-based sorbents. Lower adsorption capacity could be due to the low BET surface area, impurities in ES, and the unstable nature of ES. Some of the Ca-sorbents reported in the literature were modified with chemicals which further enhanced the adsorption capacity. No one has reported ES in the form of CaCO<sub>3</sub>. If it has been tested in the raw form maybe the reported adsorption capacity readings would be much lower compared to ES. Thus, it is expected that if ES is further modified to calcined ES, it could definitely perform better than the ones reported in the literature. The only one who has done similar work on ES is Witoon (2011) who tried for CO<sub>2</sub> capture at various temperatures by TGA method [23]. The carbonation rate was around 35% at 750 °C of calcination temperature. Thus, there is a big potential for calcined ES to be used for pollutant gases removal.

Table 7. Comparison of raw and calcined (900 °C) eggshell with other Ca-based sorbents for SO<sub>2</sub> and H<sub>2</sub>S.

Gas	Sorbent	Conditions	Adsorption Capacity/ Removal Efficiency	Ref.
SO <sub>2</sub>	Ethanol treated calcined limestone (CaO) (BET = 35.5 m <sup>2</sup> /g)	Reaction temperature = 1050 °C SO <sub>2</sub> —2000 ppm by volume Residence time = 1 s Ca/S ratio = 3	Around 55%	[52]
	Commercial Ca(OH) <sub>2</sub> mixed with rice husk ash (BET = 106.10 m <sup>2</sup> /g)	Reaction temperature—100 °C SO <sub>2</sub> = 1000 ppm NO = 500 ppm CO <sub>2</sub> = 12% N <sub>2</sub> = balance	10.72 mg/g	[53]
	Commercial Ca(OH) <sub>2</sub> mixed oil palm ash (BET = 88.3 m <sup>2</sup> /g)		5.36 mg/g	
	Commercial Ca(OH) <sub>2</sub> mixed with coal fly ash (BET = 62.2 m <sup>2</sup> /g)		4.29 mg/g	

Table 7. Cont.

Gas	Sorbent	Conditions	Adsorption Capacity/ Removal Efficiency	Ref.
	Ca(OH) <sub>2</sub> obtained from oyster shell (BET = 12.9 m <sup>2</sup> /g)—CaO content = 53.8%	Reaction temperature—150 °C SO <sub>2</sub> = 1800 ppm NO <sub>x</sub> = 250 ppm O <sub>2</sub> = 6% Water vapors = 10%	0.78 mmol/g	[54]
	Hydrated Lime (BET = 8.76 m <sup>2</sup> /g)	Reaction temperature = 70 °C NO <sub>2</sub> = 249 ppm SO <sub>2</sub> = 906 ppm Relative humidity = 60%	25% (SO <sub>2</sub> )	[55]
	Ca(OH) <sub>2</sub> mixed with fly ash in ratio of 1:3 with additional treatment with KMnO <sub>4</sub> (BET = 19.04 m <sup>2</sup> /g)	Reaction temperature = 80 °C SO <sub>2</sub> = 500 ppm NO = 200 ppm O <sub>2</sub> = 5% Relative Humidity = 80%	60–80%	[56]
	Oxidant enriched Ca(OH) <sub>2</sub> (BET = 11 to 14 m <sup>2</sup> /g)	Reaction temperature—80 °C SO <sub>2</sub> —600 ppm NO—300 ppm O <sub>2</sub> —8% H <sub>2</sub> O—10.5%	80–100 mg/g	[57]
	Calcined eggshell (BET = 6.74 m <sup>2</sup> /g)	Reaction temperature—30 °C SO <sub>2</sub> —300 ppm N <sub>2</sub> -balance Relative humidity—40%	11.68 mg/g	This work
	CaO from waste CaCO <sub>3</sub> (BET < 3 m <sup>2</sup> /g)	Reaction temperature—20 °C H <sub>2</sub> S—50 ppm in air TGA Analysis Reaction time 55 min	55%	
	CaCO <sub>3</sub> from waste (BET < 3.98 m <sup>2</sup> /g)	Reaction temperature-Ambient Biogas with 200 ppmv H <sub>2</sub> S Reaction time 400 min	85%	[10]
H <sub>2</sub> S	Dried fly ash (BET = 17.71 m <sup>2</sup> /g)	Reaction temperature-Not Given H <sub>2</sub> S—300 ppm in air	10.4 mg/g	
	Australian red soil (BET = not given)	Reaction temperature-Not Given H <sub>2</sub> S = 2000 ppm N <sub>2</sub> -balance	18.8 mg/g	
	Calcined eggshell (BET 6.74 m <sup>2</sup> /g)	Reaction temperature—30 °C H <sub>2</sub> S—300 ppm N <sub>2</sub> -balance Relative humidity—40%	7.96 mg/g	This work

### 3. Materials and Methods

#### 3.1. Sorbent Preparation

Chicken eggshell waste (brown in color classified as Grade B and C) was collected from the student's food court in the university campus. It was thoroughly soaked and washed with tap water until a clean eggshell were obtained. Two types of raw eggshell were prepared i.e., with the membrane (RES) and without the membrane. For the samples without the membrane, the membrane was carefully removed after soaking in water. The ES samples were then dried in an UF 110 oven (Memmert, Schwabach, Germany) at 105 °C for 24 h to remove the excessive moisture. Finally, the samples were ground to different particle sizes using a MX-GM1011H dry blender (Panasonic, Selangor, Malaysia). The powdered ES samples were then sieved using a WS TYLER RX29 vibrating sieve

(Fisher Scientific, Pittsburgh, PA, USA). Three different particle sizes were isolated (<90  $\mu\text{m}$ , 90–125  $\mu\text{m}$  and 125–180  $\mu\text{m}$ ). Calcined ES (CES) samples were prepared by heating the powdered RES at different temperatures (800  $^{\circ}\text{C}$ , 900  $^{\circ}\text{C}$ , 950  $^{\circ}\text{C}$ , 1000  $^{\circ}\text{C}$ , 1100  $^{\circ}\text{C}$ ) for 2 h using a LEF-103S model muffle furnace (LabTech, Debrecen, Hungary). The retention time for calcination was chosen based on preliminary studies.

### 3.2. Adsorption Tests

The adsorption tests were performed in a lab-scale adsorption reactor as shown in Figure S1 (Supplementary Material).  $\text{SO}_2$  and  $\text{H}_2\text{S}$  gas flow from the gas cylinders (2000 ppm, 99% purity) were controlled automatically using SDPROC mass flow controllers and flow meters (Aalborg, New York, NY, USA). The gas flow rates of both gases into the reactor were kept at 300 mL/min throughout the experiments.  $\text{H}_2\text{S}$  and  $\text{SO}_2$  concentrations were kept constant at 300 ppm by introducing nitrogen gas as balance. Low flowrate and concentration were chosen for the overall safety of the lab. A down-flow fixed bed reactor made of stainless steel with an internal diameter of 9 mm and a height of 180 mm was prepared to fill the sorbents. The reactor was fixed inside an oven (Mettler, Schwabach, Germany) for temperature study. In each run, 1 g of sorbent was placed inside the reactor. The initial and outlet concentrations of  $\text{H}_2\text{S}$  and  $\text{SO}_2$  gas were measured using Biogas 5000 Portable Gas Analyzer (Geotech, Chelmsford Essex, UK) and Vario-Plus Industrial Gas-Analyzer (MRU Instruments Inc., Humble, TX, USA) respectively.  $\text{SO}_2$  and  $\text{H}_2\text{S}$  analyzers recorded the gas concentrations every second. The adsorption capacity was calculated from the following equation [58] using the breakthrough curve generated during the experiment:

$$Q = \frac{C_0 M w q}{1000 w V_m} \int_0^t \left(1 - \frac{C}{C_0}\right) dt \quad (7)$$

where  $Q$  is adsorption capacity (mg/g),  $c_0$  is the initial inlet concentration (ppm),  $M_w$  is the gas molecular weight (g/mol),  $q$  is the total flow rate (L/min),  $w$  is the weight of sorbent (g),  $V_m$  is the molar volume (L/mol),  $c$  is the outlet concentration of the gas (ppm) at time  $t$  (min). The adsorption capacity calculation was based on an average of 3 repetitions of the adsorption breakthrough curve. The differences between the 3 readings were less than 3%.

### 3.3. Process Parameters Study

In the process study, the effects of the relative humidity in the inlet gas and reaction temperature were evaluated for both RES and CES sorbents. Only optimized sorbents (both RES and CES) were selected for the process study. The reactor was fixed inside the oven and the temperature of the oven was varied from room temperature (approximately 30  $^{\circ}\text{C}$ ) to 200  $^{\circ}\text{C}$  to study the effect of temperature on adsorption tests. Whereas the humidity in the inlet gas was created by passing the inlet gas through an airtight conical flask which was submerged in a temperature-controlled water bath before it could enter the reactor at room temperature. Required humidity in the inlet gas was created as the gas passing through the water bath was saturated with water vapor at the set temperature. The temperature of the water bath was set based on the steam tables formulation to create 40% relative humidity in the inlet gas. 40% of relative humidity was selected as it can be generated at room temperature and also to protect the gas sensors in the analyzer.

### 3.4. Characterization of the Sorbents

Morphology of the RES and CES were analysed by field emission scanning electron microscope (FESEM), model JEOL JSM-6701F (JEOL, Akishima City, Japan). The energy-dispersive X-ray spectroscopy (EDS) (JEOL, Akishima City, Japan) was employed to detect the specific elements on the surface of the materials. Fourier Transform Infrared (FTIR) Lambda 35 (Perkin Elmer, Waltham, MA, USA) was used to determine the surface functional groups of the sorbents. The spectra were recorded in the spectral range of 400–4000  $\text{cm}^{-1}$  with a resolution of 4  $\text{cm}^{-1}$  by mixing a small quantity of the sorbent with potassium bromide. pH was measured by preparing a solution in the ratio of 0.1 g of

sorbent in 20 mL deionized water and stirred for 1.5 hr. A digital pH meter was used (Hanna Instruments, Woonsocket, RI, USA). X-ray diffraction model Lab X XRD-6000 (Shimadzu, Tokyo, Japan) was used to identify the XRD patterns of the sorbents at room temperature at  $2\theta$  with a step size of 0.02. The Brunauer–Emmett–Teller (BET) surface area and pore size distribution were calculated using nitrogen adsorption and desorption isotherms conducted at 77 K with micromeritics, ASAP 2020 V4.02 (Micromeritics, Norcross, GA, USA) volumetric gas adsorption instrument. Thermogravimetric analysis (TGA) of RES and CES was done with TGA/DSC 3+ (Mettler Toledo, Ohio, OH, USA) for proximate analysis. Nitrogen gas was used at 20 mL/min at a heating rate of 10 °C /min until 900 °C. Original images of ES were taken with a smartphone.

#### 4. Conclusions

RES and CES sorbents were tested for SO<sub>2</sub> and H<sub>2</sub>S adsorption. It was found that RES with membrane and having the smallest particle size i.e., <90 µm showed the best adsorption capacity for both SO<sub>2</sub> and H<sub>2</sub>S. (CES 900 °C) showed the best adsorption capacity among the other calcination temperature and RES. It can be concluded that physical adsorption was dominant over the chemical adsorption for both RES and CES sorbents. The characterization study shows the existences of sulfur element in the spent adsorbents which further verifies the adsorption of SO<sub>2</sub> and H<sub>2</sub>S by CES. The presence of the relative humidity in the inlet gas and increasing reaction temperature improved the performance of both RES and CES sorbents. (CES 900 °C) showed a greater adsorption capacity compared to RES with the addition of humidity. The best adsorption capacity of SO<sub>2</sub> and H<sub>2</sub>S was recorded as 11.68 mg/g and 7.96 mg/g respectively using (CES 900 °C) with 40% RH. These results indicate that chicken eggshell have great potential to be used as sorbents upon modification for the removal of pollutant gases such as SO<sub>2</sub> and H<sub>2</sub>S from contaminated air.

**Supplementary Materials:** The following are available online at <https://www.mdpi.com/2073-4344/11/2/295/s1>, Figure S1: Schematic diagram of adsorption experimental setup.

**Author Contributions:** W.A. and S.S. contributed equally. Conceptualization, S.S. and Y.M.; methodology, R.K.; validation, R.K., Y.M., and S.S.; formal analysis, W.A. and S.S.; investigation, W.A. and S.S.; resources, S.S. and Y.M.; data curation, W.A. and R.K.; writing—original draft preparation, W.A.; writing—review and editing, W.A., S.S., R.K., and Y.M.; visualization, W.A. and Y.M.; supervision, S.S.; project administration, S.S. and Y.M.; funding acquisition, S.S. All authors have read and agreed to the published version of the manuscript.

**Funding:** This research was funded by Universiti Tunku Abdul Rahman Research Fund number UTARRF/2017-C1/S07 and the APC was funded by Universiti Tunku Abdul Rahman under Financial Support for Journal Paper Publication Scheme and the authors.

**Data Availability Statement:** Data is contained within the article or Supplementary Material.

**Acknowledgments:** The authors gratefully acknowledge the financial support received from Universiti Tunku Abdul Rahman.

**Conflicts of Interest:** The authors declare no conflict of interest.

#### References

1. Awe, O.W.; Zhao, Y.; Nzihou, A.; Minh, D.P.; Lyczko, N. A Review of Biogas Utilisation, Purification and Upgrading Technologies. *Waste Biomass Valorization* **2017**, *8*, 267–283. [CrossRef]
2. Du, E.; Dong, D.; Zeng, X.; Sun, Z.; Jiang, X.; de Vries, W. Direct Effect of Acid Rain on Leaf Chlorophyll Content of Terrestrial Plants in China. *Sci. Total Environ.* **2017**, *605*, 764–769. [CrossRef]
3. Zhang, Y.; Wang, T.; Yang, H.; Zhang, H.; Zhang, X. Experimental Study on SO<sub>2</sub> Recovery Using a Sodium—Zinc Sorbent Based Flue Gas Desulfurization Technology. *Chin. J. Chem. Eng.* **2015**, *23*, 241–246. [CrossRef]
4. Córdoba, P. Status of Flue Gas Desulfurisation (FGD) Systems from Coal-Fired Power Plants: Overview of the Physic-Chemical Control Processes of Wet Limestone FGDs. *Fuel* **2015**, *144*, 274–286. [CrossRef]
5. Qu, Z.; Sun, F.; Liu, X.; Gao, J.; Qie, Z.; Zhao, G. The Effect of Nitrogen-Containing Functional Groups on SO<sub>2</sub> Adsorption on Carbon Surface: Enhanced Physical Adsorption Interactions. *Surf. Sci.* **2018**, *677*, 78–82. [CrossRef]

6. Li, P.; Wang, X.; Allinson, G.; Li, X.; Stagnitti, F.; Murray, F.; Xiong, X. Effects of Sulfur Dioxide Pollution on the Translocation and Accumulation of Heavy Metals in Soybean Grain. *Environ. Sci. Pollut. Res.* **2011**, *18*, 1090–1097. [CrossRef] [PubMed]
7. Li, C.; Sheng, Y.; Sun, X. Simultaneous Removal of SO<sub>2</sub> and NO<sub>x</sub> by a Combination of Red Mud and Coal Mine Drainage. *Environ. Eng. Sci.* **2019**, *36*, 444–452. [CrossRef]
8. Silas, K.; Ghani, W.A.; Choong, T.S.; Rashid, U. Carbonaceous Materials Modified Catalysts for Simultaneous SO<sub>2</sub>/NO<sub>x</sub> Removal from Flue Gas: A Review. *Catal. Rev.* **2019**, *61*, 134–161. [CrossRef]
9. El Asri, O.; Hafidi, I.; elamin Afilal, M. Comparison of Biogas Purification by Different Substrates and Construction of a Biogas Purification System. *Waste Biomass Valorization* **2015**, *6*, 459–464. [CrossRef]
10. Ahmad, W.; Sethupathi, S.; Kanadasan, G.; Lau, L.C.; Kanthasamy, R. A Review on the Removal of Hydrogen Sulfide from Biogas by Adsorption Using Sorbents Derived from Waste. *Rev. Chem. Eng.* **2019**. [CrossRef]
11. Shah, M.S.; Tsapatsis, M.; Siepmann, J.I. Hydrogen Sulfide Capture: From Absorption in Polar Liquids to Oxide, Zeolite, and Metal-Organic Framework Adsorbents and Membranes. *Chem. Rev.* **2017**, *117*, 14. [CrossRef]
12. Abatzoglou, N.; Boivin, S. A Review of Biogas Purification Processes. *Biofuels Bioprod. Biorefining* **2009**, *3*, 42–71. [CrossRef]
13. Baláz, M. Ball Milling of Eggshell Waste as a Green and Sustainable Approach: A Review. *Adv. Colloid Interface Sci.* **2018**, *256*, 256–275. [CrossRef]
14. Oliveira, D.A.; Benelli, P.; Amante, E.R. A Literature Review on Adding Value to Solid Residues: Egg Shells. *J. Clean. Prod.* **2013**, *46*, 42–47. [CrossRef]
15. Food and Agriculture Organization (FAO); U.N. Livestock Production. 2015. Available online: <http://www.fao.org/docrep/005/y4252e/y4252e07.htm> (accessed on 30 August 2019).
16. Rohim, R.; Ahmad, R.; Ibrahim, N.; Hamidin, N.; Abidin, C.Z.A. Characterization of Calcium Oxide Catalyst from Eggshell Waste. *Adv. Environ. Biol.* **2014**, *8*, 35–38.
17. De Angelis, G.; Medeghini, L.; Conte, A.M.; Mignardi, S. Recycling of Eggshell Waste into Low-Cost Adsorbent for Ni Removal from Wastewater. *J. Clean. Prod.* **2017**, *164*, 1497–1506. [CrossRef]
18. Laca, A.; Laca, A.; Díaz, M. Eggshell Waste as Catalyst: A Review. *J. Environ. Manag.* **2017**, *197*, 351–359. [CrossRef] [PubMed]
19. Hosseini, S.; Eghbali Babadi, F.; Masoudi Soltani, S.; Aroua, M.K.; Babamohammadi, S.; Mousavi Moghadam, A. Carbon Dioxide Adsorption on Nitrogen-Enriched Gel Beads from Calcined Eggshell/Sodium Alginate Natural Composite. *Process Saf. Environ. Prot.* **2017**, *109*, 387–399. [CrossRef]
20. Sethupathi, S.; Kai, Y.C.; Kong, L.L.; Munusamy, Y.; Bashir, M.J.K.; Ibrahimi, N. Preliminary Study of Sulfur Dioxide Removal Using Calcined Egg Shell. *Malays. J. Anal. Sci.* **2017**, *21*, 719–725. [CrossRef]
21. Sun, Y.; Yang, G.; Zhang, L. Hybrid Adsorbent Prepared from Renewable Lignin and Waste Egg Shell for SO<sub>2</sub> Removal: Characterization and Process Optimization. *Ecol. Eng.* **2018**, *115*, 139–148. [CrossRef]
22. Cho, Y.B.; Seo, G.; Chang, D.R. Transesterification of Tributyrin with Methanol over Calcium Oxide Catalysts Prepared from Various Precursors. *Fuel Process. Technol.* **2009**, *90*, 1252–1258. [CrossRef]
23. Witton, T. Characterization of Calcium Oxide Derived from Waste Eggshell and Its Application as CO<sub>2</sub> Sorbent. *Ceram. Int.* **2011**, *37*, 3291–3298. [CrossRef]
24. Gergely, G.; Weber, F.; Lukacs, I.; Toth, A.L.; Horvath, Z.E.; Mihaly, J.; Balazsi, C. Preparation and Characterization of Hydroxyapatite from Eggshell. *Ceram. Int.* **2010**, *36*, 803–806. [CrossRef]
25. Engin, B.; Demirtaş, H.; Eken, M. Temperature Effects on Egg Shells Investigated by XRD, IR and ESR Techniques. *Radiat. Phys. Chem.* **2006**, *75*, 268–277. [CrossRef]
26. Lee, K.T.; Mohamed, A.R.; Bhatia, S.; Chu, K.H. Removal of Sulfur Dioxide by Fly Ash/CaO/CaSO<sub>4</sub> Sorbents. *Chem. Eng. J.* **2005**, *114*, 171–177. [CrossRef]
27. Zhao, Y.; Han, Y.; Chen, C. Simultaneous Removal of SO<sub>2</sub> and NO from Flue Gas Using Multicomposite Active Absorbent. *Ind. Eng. Chem. Res.* **2011**, *51*, 480–486. [CrossRef]
28. Tsai, W.T.; Yang, J.M.; Lai, C.W.; Cheng, Y.H.; Lin, C.C.; Yeh, C.W. Characterization and Adsorption Properties of Eggshells and Eggshell Membrane. *Bioresour. Technol.* **2006**, *97*, 488–493. [CrossRef] [PubMed]
29. Al-ghouti, M.A.; Khan, M. Eggshell Membrane as a Novel Bio Sorbent for Remediation of Boron from Desalinated Water. *J. Environ. Manag.* **2017**, *207*, 405–416. [CrossRef]
30. Pramanpol, N.; Nitayapat, N. Adsorption of Reactive Dye by Eggshell and Its Membrane. *Kasetsart J.* **2006**, *40*, 192–197.
31. Al-Hosney, H.A.; Grassian, V.H. Water, Sulfur Dioxide and Nitric Acid Adsorption on Calcium Carbonate: A Transmission and ATR-FTIR Study. *Phys. Chem. Chem. Phys.* **2005**, *7*, 1266–1276. [CrossRef]
32. De-Diego, L.; Abad, A.; Garcia-Lebiano, F.; Adanez, J.; Gayan, P. Simultaneous Calcination and Sulfidation of Calcium-Based Sorbents. *Ind. Eng. Chem. Res.* **2004**, *43*, 3261–3269. [CrossRef]
33. Valverde, J.M.; Medina, S. Reduction of Calcination Temperature in the Calcium Looping Process for CO<sub>2</sub> Capture by Using Helium: In Situ XRD Analysis. *Sustain. Chem. Eng.* **2016**, *4*, 7090–7097. [CrossRef]
34. Doğu, T.I. The Importance of Pore Structure and Diffusion in the Kinetics of Gas-Solid Non-Catalytic Reactions: Reaction of Calcined Limestone with SO<sub>2</sub>. *Chem. Eng. J.* **1981**, *21*, 213–222. [CrossRef]
35. Quina, M.J.; Soares, M.A.R.; Quinta-ferreira, R. Applications of Industrial Eggshell as a Valuable Anthropogenic Resource. *Resour. Conserv. Recycl.* **2017**, *123*, 176–186. [CrossRef]

36. Hartman, M.; Svoboda, K.; Trnka, O.; Čermák, J. Reaction between Hydrogen Sulfide and Limestone Calcines. *Ind. Eng. Chem. Res.* **2002**, *41*, 2392–2398. [[CrossRef](#)]
37. Borgwardt, R.H. Sintering of Nascent Calcium Oxide. *Chem. Eng. Sci.* **1989**, *44*, 53–60. [[CrossRef](#)]
38. Slack, A.V.; Falkenberry, H.L.; Harrington, R.E. Sulfur Oxide Removal from Waste Gases: Lime-Limestone Scrubbing Technology. *J. Air Pollut. Control Assoc.* **1972**, *22*, 159–166. [[CrossRef](#)]
39. Liu, C.-F.; Shih, S.-M.; Lin, R.-B. Kinetics of the Reaction of Ca(OH)<sub>2</sub>/Fly Ash Sorbent with SO<sub>2</sub> at Low Temperatures. *Chem. Eng. Sci.* **2002**, *57*, 93–104. [[CrossRef](#)]
40. Agnihotri, R.; Chauk, S.S.; Mahuli, S.K.; Fan, L.S. Mechanism of CaO Reaction with H<sub>2</sub>S: Diffusion through CaS Product Layer. *Chem. Eng. Sci.* **1999**, *54*, 3443–3453. [[CrossRef](#)]
41. Krammer, G.; Brunner, C.; Khinast, J.; Staudinger, G. Reaction of Ca(OH)<sub>2</sub> with SO<sub>2</sub> at Low Temperature. *Ind. Eng. Chem. Res.* **1997**, *36*, 1410–1418. [[CrossRef](#)]
42. Galloway, B.D.; MacDonald, R.A.; Padak, B. Characterization of Sulfur Products on CaO at High Temperatures for Air and Oxy-Combustion. *Int. J. Coal Geol.* **2016**, *167*, 1–9. [[CrossRef](#)]
43. Song, C.; Pan, W.; Srimat, S.T.; Zheng, J.; Li, Y.; Wang, Y.H.; Xu, B.Q.; Zhu, Q.M. Tri-Reforming of Methane over Ni Catalysts for CO<sub>2</sub> Conversion to Syngas with Desired H<sub>2</sub>CO Ratios Using Flue Gas of Power Plants without CO<sub>2</sub> Separation. *Stud. Surf. Sci. Catal.* **2004**, *153*, 315–322.
44. Weiland, P. Biogas Production: Current State and Perspectives. *Appl. Microbiol. Biotechnol.* **2010**, *85*, 849–860. [[CrossRef](#)] [[PubMed](#)]
45. Shi, L.; Xu, X. Study of the Effect of Fly Ash on Desulfurization by Lime. *Fuel* **2001**, *80*, 1969–1973. [[CrossRef](#)]
46. Fenouil, L.A.; Towler, G.P.; Lynn, S. Removal of H<sub>2</sub>S from Coal Gas Using Limestone: Kinetic Considerations. *Ind. Eng. Chem. Res.* **1994**, *33*, 265–272. [[CrossRef](#)]
47. Wilhelm, E.; Battino, R.; Wilcock, R.J. Low-Pressure Solubility of Gases in Liquid Water. *Chem. Rev.* **1977**, *77*, 219–262. [[CrossRef](#)]
48. Baltrusaitis, J.; Usher, C.R.; Grassian, V.H. Reactions of Sulfur Dioxide on Calcium Carbonate Single Crystal and Particle Surfaces at the Adsorbed Water Carbonate Interface. *Phys. Chem. Chem. Phys.* **2007**, *9*, 3011. [[CrossRef](#)] [[PubMed](#)]
49. Martínez, M.G.; Minh, D.P.; Nzihou, A.; Sharrock, P. Valorization of Calcium Carbonate-Based Solid Wastes for the Treatment of Hydrogen Sulfide in a Semi-Continuous Reactor. *Chem. Eng. J.* **2019**, *360*, 1167–1176. [[CrossRef](#)]
50. Ma, S.; Yao, J.; Gao, L.; Ma, X.; Zhao, Y. Experimental Study on Removals of SO<sub>2</sub> and NO<sub>x</sub> Using Adsorption of Activated Carbon/Microwave Desorption. *J. Air Waste Manag. Assoc.* **2012**, *62*, 1012–1021. [[CrossRef](#)]
51. Garcia-Labiano, F.; De Diego, L.F.; Adánez, J. Effectiveness of Natural, Commercial, and Modified Calcium-Based Sorbents as H<sub>2</sub>S Removal Agents at High Temperatures. *Environ. Sci. Technol.* **1999**, *33*, 288–293. [[CrossRef](#)]
52. Adanez, J.; Fierro, V.; Garcia-Labiano, F.; Palacios, J. Study of Modified Calcium Hydroxides for Enhancing SO<sub>2</sub> Removal during Sorbent Injection in Pulverized Coal Boilers. *Fuel* **1997**, *76*, 257–265. [[CrossRef](#)]
53. Dahlan, I.; Mohamed, A.R.; Kamaruddin, A.H.; Lee, K.T. Dry SO<sub>2</sub> Removal Process Using Calcium/Siliceous-Based Sorbents: Deactivation Kinetics Based on Breakthrough Curves. *Chem. Eng. Technol. Ind. Chem. Equip. Process Eng.* **2007**, *30*, 663–666. [[CrossRef](#)]
54. Jung, J.; Yoo, K.; Kim, H.; Lee, H.; Shon, B.-H. Reuse of Waste Oyster Shells as a SO<sub>2</sub>/NO<sub>x</sub> Removal Absorbent. *J. Ind. Eng. Chem.* **2007**, *13*, 512–517.
55. Nelli, C.H.; Rochelle, G.T. Simultaneous Sulfur Dioxide and Nitrogen Dioxide Removal by Calcium Hydroxide and Calcium Silicate Solids. *J. Air Waste Manag. Assoc.* **1998**, *48*, 819–828. [[CrossRef](#)]
56. Zhang, H.; Tong, H.; Wang, S.; Zhuo, Y.; Chen, C.; Xu, X. Simultaneous Removal of SO<sub>2</sub> and NO from Flue Gas with Calcium-Based Sorbent at Low Temperature. *Ind. Eng. Chem. Res.* **2006**, *45*, 6099–6103. [[CrossRef](#)]
57. Ghorishi, S.B.; Singer, C.F.; Jozewicz, W.S.; Sedman, C.B.; Srivastava, R.K. Simultaneous Control of Hg<sup>0</sup>, SO<sub>2</sub>, and NO<sub>x</sub> by Novel Oxidized Calcium-Based Sorbents. *J. Air Waste Manag. Assoc.* **2002**, *52*, 273–278. [[CrossRef](#)] [[PubMed](#)]
58. Ibrahimi, N.; Sethupathi, S.; Bashir, M.J.K. Optimization of Palm Oil Mill Sludge Biochar Preparation for Sulfur Dioxide Removal. *Environ. Sci. Pollut. Res.* **2018**. [[CrossRef](#)]